



OTC 6636

## Assessment of the Blast Resistance of Offshore Toppers Structures

S. Walker, Chunsheng Hu, and J.R. Williams, Wimpey Offshore

Copyright 1991, Offshore Technology Conference

This paper was presented at the 23rd Annual OTC in Houston, Texas, May 6-9, 1991.

This paper was selected for presentation by the OTC Program Committee following review of information contained in an abstract submitted by the author(s). Contents of the paper, as presented, have not been reviewed by the Offshore Technology Conference and are subject to correction by the author(s). The material, as presented, does not necessarily reflect any position of the Offshore Technology Conference or its officers. Permission to copy is restricted to an abstract of not more than 300 words. Illustrations may not be copied. The abstract should contain conspicuous acknowledgment of where and by whom the paper is presented.

### ABSTRACT

This paper describes the methodology used to assess the blast resistance capacity of compartments of existing and proposed offshore structures. Unlike previous work published in this area the emphasis is on structural assessment of whole compartments including load bearing walls, floors and ceilings. Methods of determining reaction and dynamic pressure loads on equipment and primary steelwork are described.

Practical guidance is given on the interpretation of existing structural codes for the assessment of existing structures and the design of new structures.

Design charts are given which enable the dynamic response of structural components to be calculated for selected pressure time histories. The response may involve deflections in the elastic, elastic/plastic and purely plastic regimes. The components may be under an imposed static loading (either in-plane or out-of-plane) during the explosion.

### INTRODUCTION

Blast walls are usually designed to deform plastically and act predominantly in bending to minimise the effect on the primary structural members of the platform. A great deal of effort is usually expended in designing the edge connections of the blast wall so that the reaction loads are transmitted to the supports without damage to the supporting steelwork. Because of the inertia of the wall it is possible to design these connections such that the transmitted shear forces and moments are much less than the peak overpressure force times the area of the wall.

Purpose-built blast walls are usually free standing and are not an integral part of the supporting structure. There are a number of references [1,2,3] which deal with the dynamic response of free standing blast walls.

Many older modules were not in fact designed against blast loading at all, or rather optimistic peak pressure levels were assumed (0.1 bar or 10 kN/m<sup>2</sup>). Outmoded venting formulae were often used [4,5] which have been shown to grossly underestimate the expected peak overpressures as they do not take account the effect of obstacles and flame acceleration effects in large enclosures. It may also have been assumed that immediate pressure release would occur due to cladding connection failure. In many cases the proximity of adjacent compartments, the inertia of the cladding, blockage by piping and equipment and the high rate of volume generation make cladding failure ineffective. In fact some cladding attachment systems have been found to have a higher capacity than the design pressure used for blast walls in the same compartment, although plastic design methods often indicate a higher blast resistance for these walls than was previously expected.

It is useful at this stage to briefly review the conventional method of free standing blast wall evaluation in order to discuss the extensions of the method necessary to evaluate compartment resistance. This is covered in the next section.

### BLAST WALL ASSESSMENT

There are a number of simplified methods available for the evaluation of blast resistance in the literature [1,6,7] as well as more direct methods of calculation using complex finite element codes. Preferred methods

References and figures at end of paper

incorporate non-linear, finite deflection and dynamic effects. Attention will be focussed on Biggs' method [1] which is implemented using a semi-analytic approach able to incorporate general resistance behaviour and general loading time histories through a non-linear oscillator model.

Biggs' method requires two basic inputs, the resistance/displacement or R/X curve and an idealised loading time history. R/X curves may be derived using large deflection, non-linear structural analysis methods.

The first step is to determine the possible failure modes of the wall which may include panel failure, stiffener failure and whole wall failure. Each mode corresponds to a different plastic hinge, or yield line pattern. Local and torsional buckling of stiffeners and wall plate may also occur before plastic hinge formation. The failure mode corresponding to the lowest ultimate resistance is the critical failure mode of the wall. The resistance will also depend critically on the edge support conditions assumed which may in turn depend on the form of loading. High pressure loading on adjacent panels may give rise to clamped edge conditions between panels even though the panels would not otherwise merit this approach. Tension and membrane effects often indicate an increased resistance but the restraint from the surrounding structure, through inertia or stiffness, may not be sufficient for these effects to be mobilised.

The resistance/displacement (R/X) curve for the component is then constructed (see figure 1). In the simple case of a panel, a representative point is selected (usually at the panel centre) to characterise the panel deflection. Following the elastic phase of deformation, there is an intermediate stage in the deformation of a panel associated with the formation of the first yield lines at the edge of the panel whilst there is still some elastic energy retained as a result of the curvature of the panel. The effective stiffness up to the plastic range may then be calculated, given the slopes of the elastic and elastic/plastic parts of the curve on the basis of equal energy absorption represented by the area under the R/X curve. A yield line analysis [1,10,11] may then be performed to determine the ultimate resistance  $R_m$  of the panel. The resistance/displacement curve shown in figure 1 may then be built up. The curve may also be built up more rigorously by the use of a finite element model of the panel, component or indeed the whole wall.

The effective mass of the wall is then calculated. This is available for simple geometries from tables [1] or by the application of simple transformation factors. These factors represent the extent of participation of the component masses associated with a mode of vibration similar in shape to the expected deflected shape of the wall under blast loading. The natural period of this mode of vibration then characterises the dynamic response of the structure.

A non-linear mass spring system may then be constructed to represent the structure as shown in figure 1.

The equations of motion for the three phases of response may then be written:-

1. elastic and elastic/plastic phases ( $X < X_e$ )

$$M_e \ddot{X} + K_e X = F_e(t) \dots \dots \dots (1)$$

2. plastic phase ( $X_e < X < X_m$ )

$$M_e \ddot{X} + R_m = F_e(t) \dots \dots \dots (2)$$

3. elastic rebound phase ( $X < X_m$ )

$$M_e \ddot{X} + [R_m - K_e (X_m - X)] = F_e(t) \dots \dots \dots (3)$$

where  $M_e$  is the effective mass of the component  
 $K_e$  is the effective stiffness  
 $F_e(t)$  is the instantaneous effective force at time  $t$   
 $X$  is the displacement of a characteristic point  
 $X_e$  is the effective elastic limit displacement for the component

A numerical time stepping technique may then be used to trace the time history of the response with the stiffness varying as determined by the R/X curve using the appropriate equation of motion for the phase of response using the final values from the previous phase as initial conditions (see figure 1). The natural period of the system in the elastic range "T" is given by:-

$$T = 2\pi \sqrt{(M_e/K_e)} \dots \dots \dots (4)$$

Design charts similar to that given in figure 4 are available for the calculation of peak response  $X_m$  given the load to natural period ratio ( $\tau$ ) and the ratio of peak overpressure  $P_m$  to component ultimate plastic resistance ( $\Gamma$ ) for a number of simple load time histories [1]. Given values of  $\Gamma$  and  $\tau$  the range of response in terms of the effective yield displacement  $X_e$  may be found. The lower region shown white corresponds to a maximum response  $X_{max}$  less than  $X_e$  and is broadly the elastic regime. The ratio  $X_{max}/X_e$  is often referred to as the ductility factor  $\mu$ . The other regions correspond broadly to responses in the ranges indicated. Displacements of these magnitudes are "acceptable" for members of different types and functions as given in table 2. There is no firm agreement between the codes [6,7,16] on suitable values and the table has been constructed based on standard practice at the time of writing. Displacements in the black, forbidden region of figure 4 are not acceptable under any circumstances ( $X_{max} > 30 X_e$ ).

Typical member and blast wall natural periods are given in table 3. It can be seen that the typical range of period ratios of interest is between 1 and 12 for an internal explosion.

The resistance and natural period of the member depend critically on any applied in-plane and out-of-plane loads. For structural walls, floors and ceilings, extensions of the method are therefore required.

### COMPARTMENT BLAST LOADS

The typical compartment considered in this paper is shown in figures 2 and 3. Table 1 gives the relevant dimensions, weights and loads for this compartment. An explosion with peak overpressure of 0.7 bar is assumed to occur in the lower compartment which is open on the west side and supports another module of similar size and weight on four points bearing on the top chord (see figure 3). The module is of conventional construction with cladding attached to a steel frame of primary steelwork.

It is interesting to note that during the explosion there appears to be an out of balance lateral force on the module equal to the difference in the blast load on the vented and unvented sides. The situation is complicated by loads on internal equipment transferred to the module wall and the force needed to accelerate the gas through the vent. Considering the module as a whole, acting as a rocket, the reaction force will be related to the momentum flux of the gas expelled. For 0.7 bar overpressure 6500 Kg of gas are ejected per second with a velocity in excess of 500 m/s giving a peak reaction force of 360 tonnes. This could have consequences for pipe runs between modules.

In some situations the floor of the module above may form the ceiling of the lower compartment, in which case the blast loads may cause the upper module to lift off and re-establish contact with increased force after the blast on the damaged and buckled structure below.

Before the blast, the compartment walls are in compression due to the dead weight of the module above. For design it is not necessary to take into account installation or extreme wind loads in combination with the blast loads. There are also out-of-plane loads on the floor due to the weight of equipment within the module.

The primary and secondary structure of the module is indicated in Figure 2. Typical methods of construction are assumed which give a steel-weight of about 500 tonnes of which 110 tonnes is cladding, grating and floor plate. The floor steel weight has been estimated to be about 140 tonnes. The effect of the equipment and piping is to increase this weight by a factor of 3.6 which increases the floor natural period from 12 to 25 milliseconds. The effect of the equipment loads is to impose a blanket load of the order of 12 kN/m<sup>2</sup> (equivalent to .12bar overpressure). The total dead load on the floor takes the main transverse members to a displacement close to one tenth of the ultimate effective yield displacement. This also has a large effect on the peak dynamic response and stresses in the floor during the blast.

For an internal explosion within the compartment, it is possible to approximate the blast loading on the walls as a uniform pressure load with a duration of 100 to 600 milliseconds\* and with a time variation which follows an isocoles triangular shape as shown in figure 3. This loading differs considerably from that resulting from an external explosion or from a high explosive detonation which is of much shorter duration and also may have a suction phase associated with shock wave generation. Loading determination is not

the subject of this paper [6,7,8,9]. There are in fact a number of identifiable peaks which will contribute to this pressure time history, but in the most severe situations the overall shape is often predominantly uni-modal as shown. The load duration is assumed to be 200 milliseconds. Determination of this load may only be achieved with any confidence by the use of numerical simulations; details may be found in [8].

During the explosion the upward force on the ceiling of the lower compartment, assuming rupture does not occur, will reduce the compressive load in the walls. The explosion will in fact put the wall into tension with loads typically equal to three times the design dead load. It is assumed that most of the pressure load on the cladding is transferred to the secondary and primary steelwork at least during the initial phase of the explosion, taken to be the first 150 milliseconds. The inertia of the cladding may ensure this even if the fixings fail subsequently.

The gas flow within the module may reach velocities of 500m/s giving rise to a dynamic pressure or drag load on piping, equipment and supporting columns. This load will be in phase with the flow velocities and will typically occur later than the peak overpressure and may be locally increased due to flow confinement between obstacles. The highest velocities will usually occur near the vents. The loads may be estimated from the local velocity field using the drag term of the Morison equation [15]. These drag loads will be transferred into shear at the equipment and piping support points mostly at floor level. Little information is currently available on "inertia" effects due to gas acceleration.

### COMPARTMENT ASSESSMENT - METHODOLOGY

The assessment of compartment blast capacity differs in three major respects from the blast assessment of free-standing blast walls:

1. Loads are transferred between walls, floors, ceilings and equipment. Membrane and tension loads may be applied from loaded, connected surfaces.
2. The fixity conditions at the edges of walls, floors and ceilings may be changed by loading on connected structures. Pinned boundary conditions may replace simply-supported and clamped edges may be more representative as a direct result of the loading on connected structures.
3. Out-of-plane static loads will be induced in floors (and ceilings) due to the presence of equipment and piping.

The overall method of analysis of the walls and floors of the compartment is shown in figure 5. The main stages of the assessment are as follows:-

1. Determine the behaviour of in plane loads in the walls and out of plane loads during the explosion. Often loads on a compartment ceiling will serve to reduce or reverse wall in-plane loads.
2. Determine the appropriate fixity conditions for panels strips and the whole wall for use in the

dynamic response analysis. A global modal analysis will give the appropriate natural periods for the components if fixity is intermediate between clamped and pinned.

3. For stiffened plate construction, determine the effective width of wall plate for each major stiffener from codes such as [12,13]. This represents the unbuckled part of the wall plate which acts with the major stiffening. Each major stiffener must be classified as plastic, compact, semi-compact and slender in order to assess whether a full plastic moment can be developed and maintained and whether there is sufficient rotation capacity for the hinge. In view of the magnitude of the pressure loading, even vertical stiffeners may be considered to be beams under combined axial loads rather than columns under lateral load.

4. Primary structural members must then be checked for local and lateral torsional buckling under dead and blast loads. If the member is found to buckle locally, then some estimate of the post buckled strength must be made so that the member may be represented in the computer model. Where indicated, buckling will occur before stresses in extreme fibres reach yield and full through section plastic hinging will not develop for these members.

5. Members which do not buckle may eventually develop plastic hinges (yield lines for panels). The plastic hinge moment capacity of a section will be reduced by axial loads whether compressive or tensile. There is a further change of member capacity associated with the deflection of the beam and the secondary moment about the hinge of the axial load. This "P -  $\delta$ " effect is beneficial if the member is in tension.

6. In order to fully develop the R/X curve for the member, floor or wall, it is necessary to account for the change of stiffness of the member in the elastic phase of deformation. Formulae for the reduction of lateral stiffness of beams are discussed later and are available in [10,11]. Membrane and tension effects for beams and plates may be incorporated into the R/X curves by reference to [10,11] if edge restraints are sufficient to mobilise them.

7. The natural periods of walls, floors, panels and major members are then determined. Any associated masses must be included and the effect of in-plane and out-of-plane loads taken into account. In the case of floors most of the mass is often in the form of equipment. In walls under axial compression loads approaching the Euler buckling load, the natural period is much longer than that for the unloaded wall.

8. Given the R/X curves and the natural period, the dynamic response may then be calculated for example using the method described previously. Values of peak dynamic displacement provide dynamic load factors in the elastic range for application to the stresses obtained from a conventional static elastic analysis of the module. If plastic deformation is indicated then the analysis will indicate any displacement limitation problems and indicate the magnitude of any permanent plastic deformations for use in the post damage analysis. In addition, the calculated plastic deformation may be used to check

whether the rotation angles of plastic hinges or yield lines have exceeded the limiting values for the member.

9. The dynamic response analysis will also supply estimates of the reaction loads at the ends of major members and around panel perimeters in conjunction with tables in references [1,11]. Dynamic reaction loads are limited by plastic failure of the member and may be reduced due to the member's inertia. Full knowledge of the support reactions may only be gained from a full elastic/plastic dynamic analysis. It is also necessary to consider reactions during the elastic rebound phase which will be in a direction opposing the blast. This aspect is important if the fixings are designed to resist loading predominantly in the blast direction. These reactions enable the shear resistance of the supports to be checked.

10. An explosion will rarely occur without a following fire and often a fire will precede an explosion. It is therefore necessary to consider the loss of strength of the structure at elevated temperatures in the determination of compartment blast resistance. It is also necessary to consider the post blast situation of the structure under dead loads with reduced strength and stiffness and with the plastic deformations of the structure modelled.

#### THE EFFECT OF OUT-OF-PLANE LOADS (floors and ceilings)

This effect may be dealt with by modifying the resistance functions. The initial displacement and the ultimate plastic resistance may be shifted, corresponding to the loading condition.

Alternatively the static load may be represented explicitly in the total loading and the response calculated as before. This alternative approach is not pursued in the following.

Assuming that the floor has an ultimate resistance  $R_m$  and an effective yield displacement  $X_e$ , the ratio of static displacement  $X_s$  to yield displacement  $X_e$  'α' may be defined by:-

$$\alpha = X_s/X_e \dots \dots \dots (5)$$

Assuming that the floor is still in the elastic regime before blast loading this parameter may also be defined in terms of the effective static load  $F_s$  and the ultimate resistance by:-

$$\alpha = F_s/R_m \dots \dots \dots (6)$$

(This assumes that the effective stiffness to effective yield is equal to the effective stiffness in the elastic range. This is approximately correct so long as the elastic-plastic region is not too extensive.)

Figure 6 shows the situation and the effect that out-of-plane static loads have on the parameters defining dynamic response. The two left hand curves show the input resistance/displacement curves for the situation where there is no static load. The force/time curve shows a peak pressure load of  $P_m$  with an isoceler triangular time history with duration  $t_d$ .

The top right hand curve of the figure shows how the R/X curve is modified by a static load of  $F_s$  leaving that portion of the resistance available to resist pressure loading of magnitude  $R_m'$  [7]. There is also a pre-existing static deflection  $X_s$  which then reduces the available deflection to effective yield to  $X_s - X_e$ . The loading curve is given below in the figure.

The modified resistance function is shown in the lower part of Figure 6.

If this modified resistance curve is input to the non-linear oscillator software described earlier, the resulting peak displacement output from the software may be corrected for the presence of the static load  $F_s$  by the simple transformation below:-

$$X_m = X_m' + X_s \dots \dots \dots (7)$$

where  $X_m'$  is the value of peak displacement output by the software resulting from the modified R/X function and a load function of the standard form given on the left of figure 6. The ratio of peak pressure to modified resistance  $R_m'$  ( $\Gamma'$ ) must also be corrected as below:-

$$\Gamma = \Gamma' (1 - X_s/X_e) \dots \dots \dots (8)$$

where  $\Gamma'$  is the value output by the software. The actual duration ratio  $\tau$  for the actual natural period must be used taking into account the masses associated with the static loading.

$X_m'$  and  $\Gamma'$  may be read from a design chart such as the one given in figure 4 and the corrections applied directly to these values.

This approach assumes that the peak deflection corresponds to the first peak of response after the load peak. This will apply to loaded floors with positive  $F_s/R_m$  ratios. For ceilings heavily loaded in a direction opposing the pressure, the peak deflection may occur during the 'rebound' phase, normally after the pressure load has subsided. In this case the direct application of the load time history, including the static component, will give the value of the peak (negative) displacement.

Figure 7 was obtained by direct calculation and shows the dynamic response of a floor with static loading equal to one tenth of the ultimate resistance. This is the situation present in the "test case" module shown in figures 2 and 3. The response can only safely be assumed to be elastic for peak pressures less than half of  $R_m$  in this case.

Achievement of the elastic limit deflection is often a suitable failure criterion for floors in view of the catastrophic consequences which would result from large plastic deformations. The response shown in figure 7 is very sensitive to peak pressure for loading periods longer than twice the floor natural period.

In contrast, figure 8 shows the response of a ceiling loaded to one third of  $R_m$  under blast loading from below. The response is reduced as expected and the structural response remains elastic under a peak pressure equal to  $R_m$ .

THE EFFECT OF IN-PLANE LOADS (walls)

There are two major effects of a simultaneous axial load on the resistance-deflection curve of a member:

1. Reduction of ultimate resistance (plastic moment) regardless of whether the axial force is tensile or compressive.
2. Decrease of the elastic stiffness if the axial force is compressive, and an increase if tensile.

Figure 9 shows the relationship between stiffness and applied compressive axial forces for a simply supported and a fixed-end beam [10]. The ordinate is the ratio of the stiffness (K) with the compressive axial force to the stiffness ( $K_0$ ) without an axial force [10]. The abscissa is a parameter proportional to the square root of the applied compressive force P, given by:

$$\sqrt{\frac{PL^2}{EI}} \dots \dots \dots (9)$$

where L is the span, E is Young's Modulus and I is the second moment of area.

For a simply supported beam, this parameter is equal to  $\pi$  times the square root of the ratio of the applied load to the Euler buckling load  $P_{cr}$  :

For a fixed-end beam, this parameter is equal to  $2\pi$  times of the square root of the ratio of the applied load to the Euler buckling load  $P_{cr}$ :

From Figure 9, it can be seen that axial compressive forces can significantly reduce the stiffness. For example, for an compressive load equal to a quarter of the critical load the stiffness coefficient reduces to 0.76 times of the original value; for half of the critical load, the stiffness coefficient reduces to half of the original value.

Plastic hinging in a section is characterised by the presence of yield stresses on either side of the plastic neutral axis. The subsequent application of an axial load to the member results in a shift of the neutral axis in order for the section to remain in equilibrium. This shifting of the axis always results in a reduction of the plastic moment of the section whether the axial load is tensile or compressive.

The application of a compressive axial load to the ends of a member which is already deforming laterally under blast loads results in an applied moment at the hinge due to the loads excentricity. For compression, this further reduces the moment capacity available to resist the blast loading.

Both the above effects must be accounted for in the calculation of ultimate resistance.

For the test case considered the upper module possesses gravitational potential energy. Any lowering of the support points of this module will result in a release of some of this gravitational energy which will be a further source of energy to be

absorbed by the deformation of the walls of the lower module. The result of this is a net increase of plastic deformation where it occurs, this may be represented by a further reduction in ultimate capacity of the walls of the lower module.

Once the stiffness coefficient and the ultimate resistance have been obtained the R/X curves may be derived. Figure 10 shows representative R/X curves for a beam. The figure shows that, as the axial compressive load increases, the ultimate resistance drops, the stiffness reduces and the elastic limit deflection increases. The compressive load therefore generally weakens the structure's blast resistance. The natural period of the component will also be modified by the presence of the axial load. A compressive load will increase the natural period bringing it closer to the blast load duration and hence potentially increasing the peak deflection. An in-plane tension will decrease the natural period.

Two methods of calculating the natural period of a member under in-plane loading are available. Firstly the stiffness may be obtained for the member including in-plane load effects following the approach described in this section. This modified stiffness may then be incorporated into the natural frequency calculation. Alternatively, the natural period may be derived directly from the differential equation of motion for a beam [2].

If these modifications are made to the input to a non-linear response program then the dynamic response for a member under in-plane loads may be calculated in the usual way. The displacements output will now be normalised in terms of the modified effective yield displacement which is known.

#### FURTHER CONSIDERATIONS

Dials, valves, tools and other objects may become detached during the blast giving rise to secondary projectiles. The projectile resistance of the walls must then be checked locally and globally. Energies up to 25Kj are possible for these secondary projectiles. Primary projectiles such as parts of exploding vessels and compressor rotor blades are often eliminated from consideration on the basis that the shut down systems will operate to prevent their generation [14].

The original design of penetrations, doors and hatches in blast walls will often have been performed statically to ensure that the resulting section properties are unchanged or stiffer than the original wall. In a dynamic sense, however, this may not be sufficient especially if large displacements are involved. Piping perpendicular to a wall will be severely loaded during wall response, the presence of this piping may also limit the allowable displacement of the wall. Penetrations should be designed to be fire proof after an explosion.

Care must be taken in interpreting the results of the analyses described in this paper. There is a great deal of uncertainty in the assumptions relating to the magnitude and form of the blast loading. In any case the loading is the result of a hypothetical combination of events which represents one of a large number of probable combinations. In addition the response charts show extremely unstable regions representing large variations in response for small

changes of the input parameters. Failure criteria adopted must reflect these uncertainties.

#### CONCLUSIONS

The main aspects of compartment blast assessment have been described.

A method has been described which enables existing design charts to be used to take into account the effect of both in-plane and out-of-plane loads on the dynamic response of structures.

#### REFERENCES

1. J.M. Biggs: Introduction to Structural Dynamics, 1964, McGraw Hill.
2. R.W. Clough and J. Penzien: Dynamics of Structures, McGraw Hill, 1975.
3. D.H. Groeneveld and P.C. Goudswaard: Implementation of Blast Resistance Requirements on Offshore Installations, Offshore Operations Post Piper Alpha, Conference held at I.Mar.E. 6 - 8 February 1991.
4. J. Singh: Sizing Vents for Gas Explosions, The Chemical Engineer, September 1979.
5. Guide for Venting of Deflagrations, NFPA 68, 1988.
6. Design of Structures to Resist the Effects of Atomic Weapons, U.S. Army Corps of Engineers Manual, EM 1110-345-415., ASCE 42, 1957
7. Structural Analysis and Design of Nuclear Plant Facilities, ASCE 58, 1980.
8. Review of The Applicability of Predictive Methods to Gas Explosions In Offshore Modules, British Gas plc, for Department of Energy, Report No. OTH 89 312.
9. A.C. van den Berg, C.J.M. van Wingerden, J.P. Zeeuwen and H.J. Pasman: Current Research at TNO on Vapour Cloud Explosion Modelling, International Conference on Vapour Cloud Modelling, 1987.
10. W.C. Young: Roark's Formulas for Stress and Strain, Sixth Edition 1989, McGraw-Hill.
11. S. Timoshenko and S. Woinowsky-Kreiger: Theory of Plates and Shells, McGraw Hill, 1989, 2nd. edition.
12. Steel, Concrete and Composite Bridges Part 3, Code of Practice for the Design of Steel Bridges, BS 5400, British Standards Institute, 1982.
13. Structural use of Steelwork in Building, Part 1, BS 5950, British Standards Institute, 1985.
14. Baker W.E., Cox P.A., Westine P.S., Kulesz J.J. and Strehlow R.A., "Fundamental Studies in Engineering 5: Explosion Hazards and Evaluation", Elsevier 1983.
15. C.A. Brebbia and S. Walker: Dynamic Analysis of Offshore Structures, Newnes - Butterworths 1980.
16. CIA - Guidelines for the design of category 1 (Blast Resistant) Control Buildings, Chemical Industry Association, 1976.

Table 1 First Generation Module - dimensions and loads

Width	13m		
Length	32m		
Height	10m		
Overpressure	0.7 bar (71 kN/m <sup>2</sup> )		
Surface	Area (m <sup>2</sup> )	Weight (T)	Direct Blast Force (kN)
North Wall	320	81	22,691.2
South Wall	320	81	22,691.2
West Wall	130	23	0 (vented)
East Wall	130	43	9,218.3
Floor	416	134	29,500.0
Total steel weight	525 Tonnes		
Total equipment weight (operating)			495 Tonnes

Table 2 Typical Allowable Displacements

Ductility Factor $\mu = X_{max}/X_e$	Component Description
1.0	Primary Structure, supporting walls
1.0	Columns in compression
1.0	Floor primary members
1.5	Secondary members
5.0	Beams - free standing walls
12.0	Beams failing in flexure [6]
20.0	Beams (local and buckling prevented)
20.0	Compact beam sections [7]

Table 3 Typical Component Natural Periods and Failure Pressures

Natural period (milliseconds)	Component Description
50	Vertical stiffener/column - pinned
25	Vertical stiffener/column - clamped
60 - 100	Blast wall panel
50	Whole wall (free standing)
25	Fully loaded floor
<b>Failure Pressures (millibar)</b>	
500 - 800	Blast wall panel
650 - 700	Strip between vertical stiffeners
200 - 400	Whole wall yield line failure
1000 - 1800	Floor (elastic failure)

n.b. Typical load durations for an extreme event internal explosion in large module are in the range 100 to 600 milliseconds (more often 200 to 400 milliseconds).

All components are assumed 50D steel.

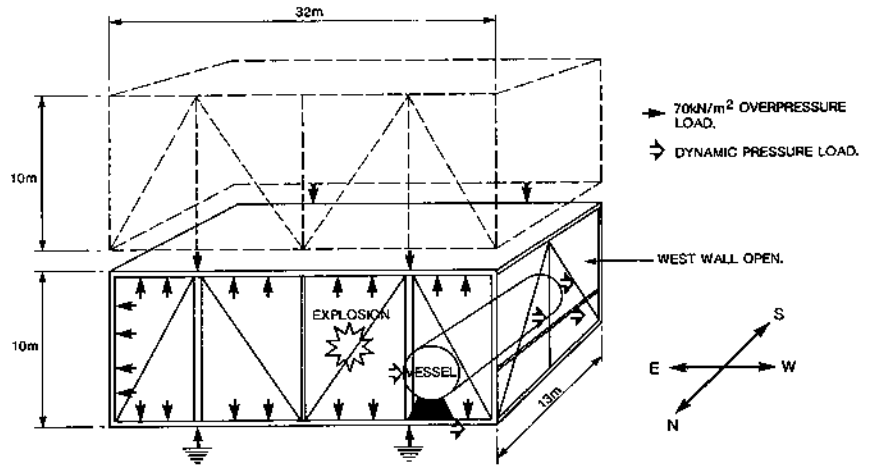


Figure 2 Compartment Loading and General Layout

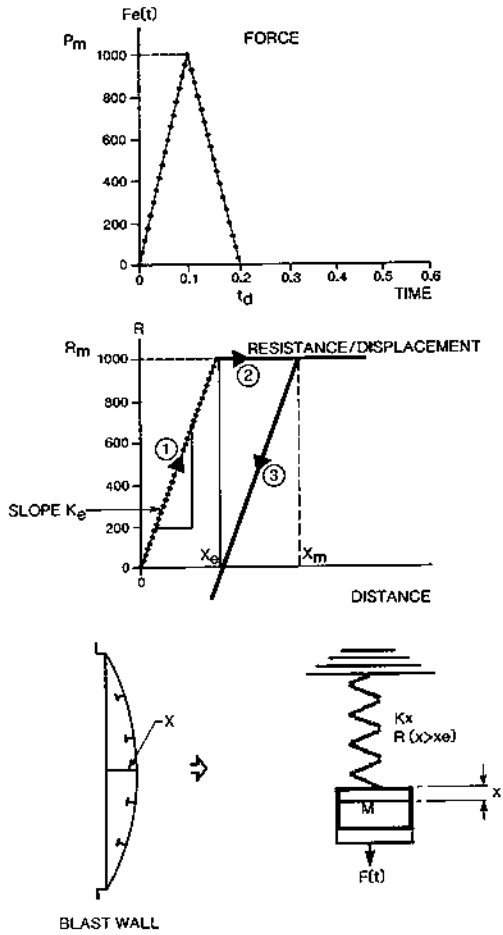


Figure 1 Non - Linear Oscillator Model

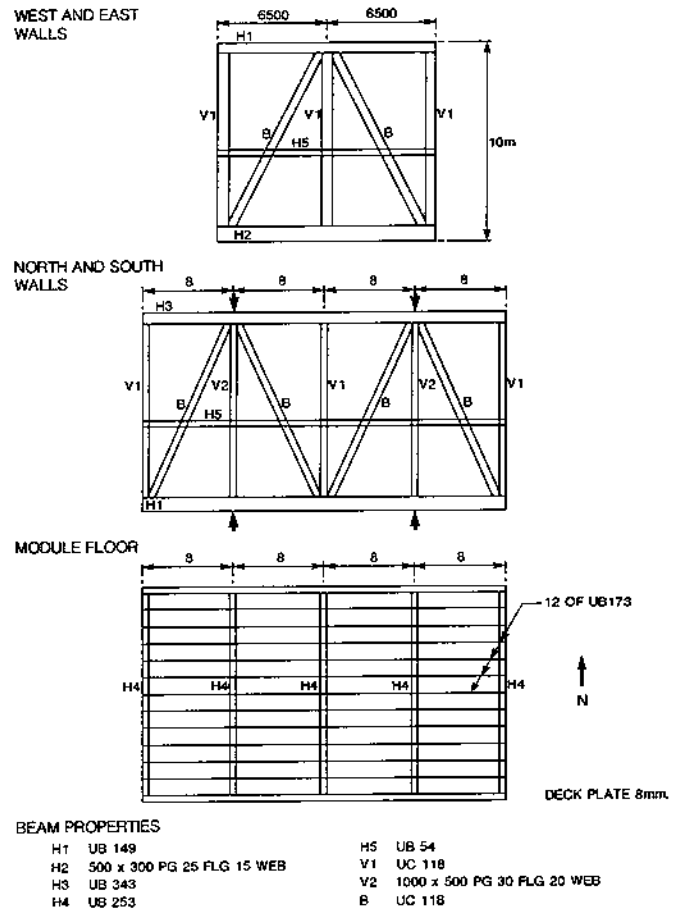


Figure 3 Compartment Simplified Structural Description

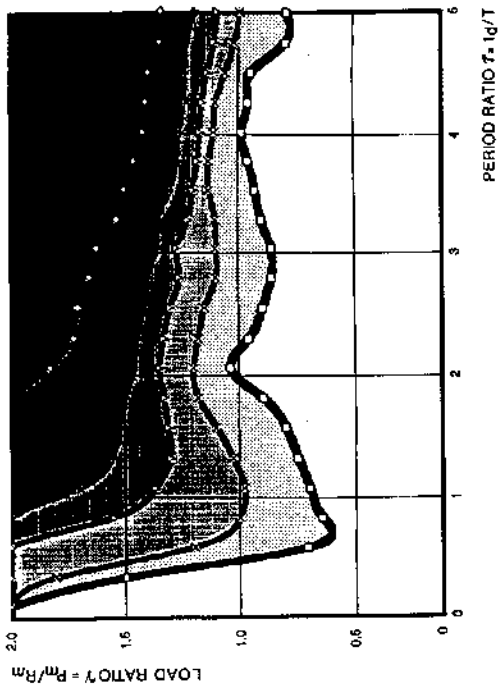


Figure 4 Design Chart - Zero Static Load

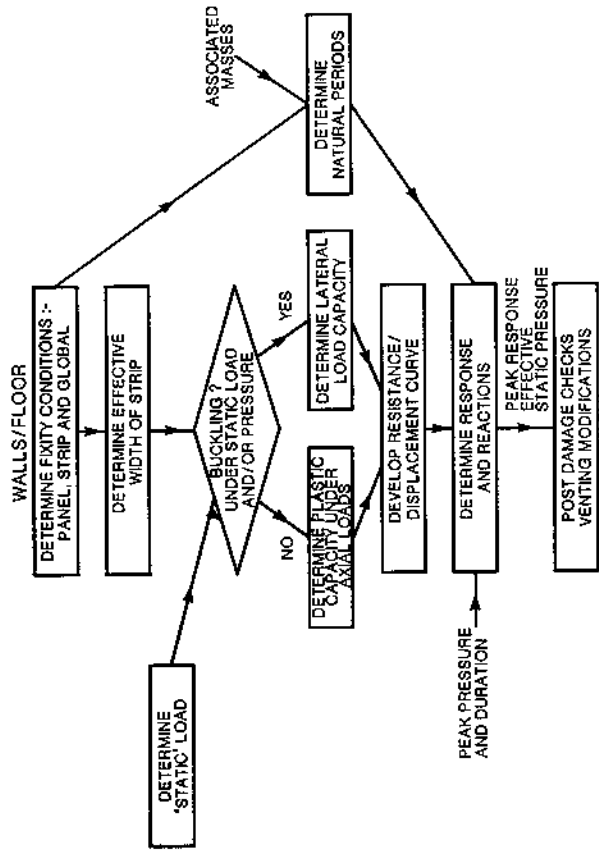


Figure 5 Blast Assessment Method

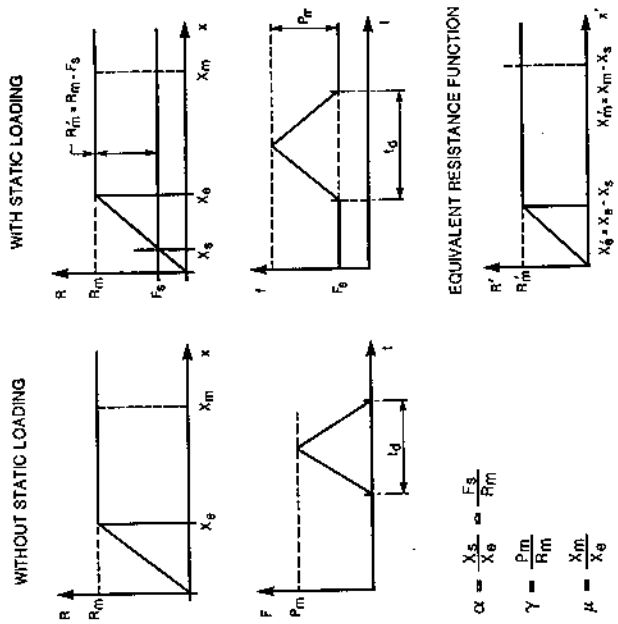


Figure 6 Out of Plane Static Loading - Notation

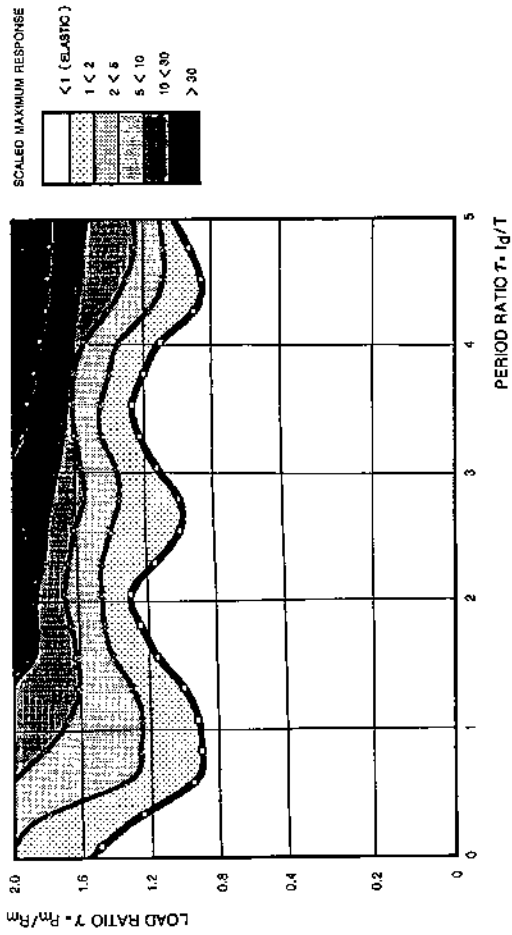


Figure 8 Design Chart - Static Load = -0.9Rm

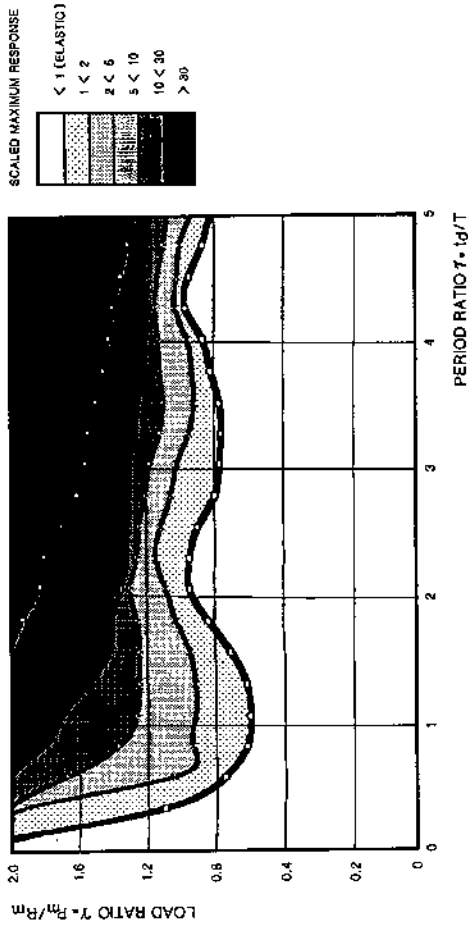


Figure 7 Design Chart - Static Load = -0.1Rm

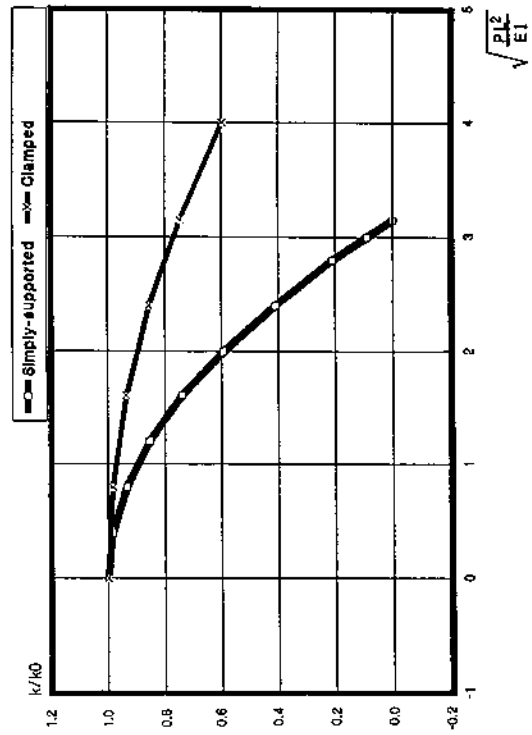


Figure 9 Stiffness Coefficients for Beams Under Combined Axial and Transverse Loads

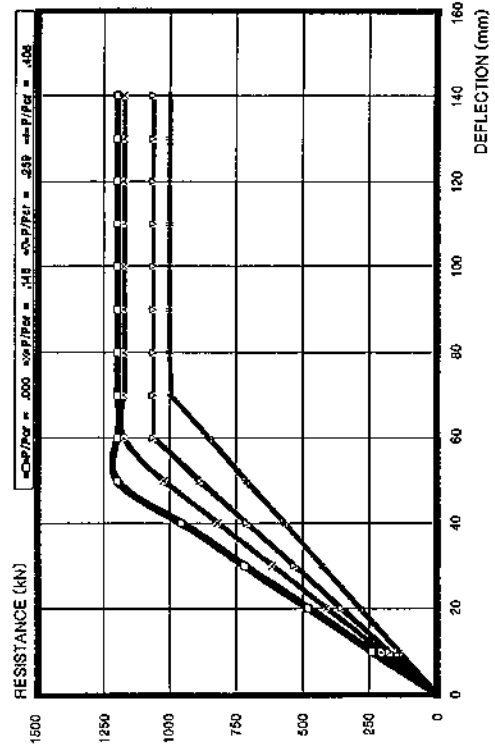


Figure 10 Resistance - Displacement Curves of a Simply Supported Beam